

Biological Scanning Electrochemical Microscopy and Its Application to Live Cell Studies

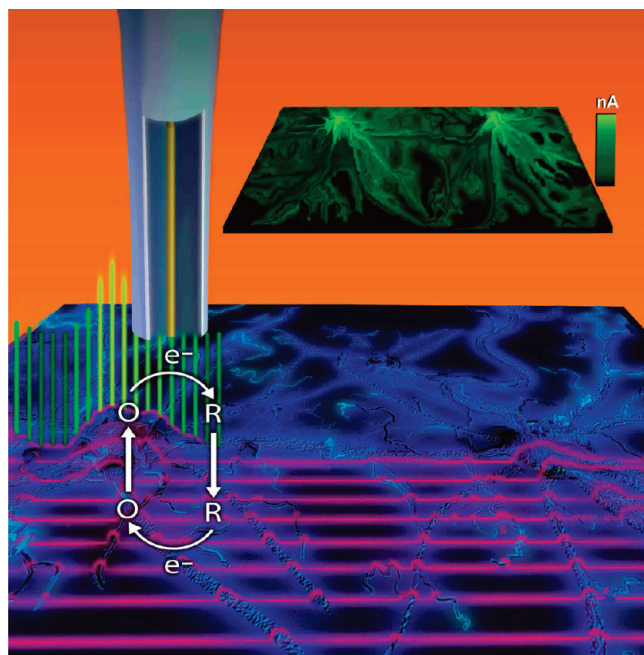
Progress in instrumental design continues to pave the way for high-resolution, real-time electrochemical measurements with living cells.

Isabelle Beaulieu, Sabine Kuss, and Janine Mauzeroll

University of Québec in Montréal (Canada)

Matthias Geissler

National Research Council of Canada



Artistic representation of Bio-SECM by Robert Gates

Scanning electrochemical microscopy (SECM) is an analytical technique that can be used to monitor electrochemical activity of a surface.^{1–3} The key element of SECM is a small-scale electrode—commonly referred to as ultramicroelectrode (UME)—that serves as a mobile probe, recording changes in electrochemical potential with remarkable sensitivity, short response times, and high spatial resolution. Since its inception by Bard and coworkers,¹ SECM has evolved to a decent level of maturity, and various proof-of-concept demonstrations have showcased many of its technical abilities. Although SECM originated in electroanalytical surface science, this technique has attracted increasing attention for biological applications and the study of living organisms. Biological SECM could possibly 1) quantify the flux of molecules entering or leaving a cell, 2) probe local electrochemical reactions occurring at or inside a cell, and 3) perform duplicate measurements on both a single cell (or portions of it) and confluent assemblies or tissues. Moreover, SECM measurements combined with other biosensing

techniques can conduct and monitor multiple experiments simultaneously on a living object. The objective of this Feature is to provide a short review of SECM with a particular emphasis on live cell studies. We outline the basic concepts underlying this technique, describe the current state of instrumentation, and highlight recent selected demonstrations deriving from the open literature.

FUNDAMENTALS

UMEs are electrochemical sensors that have dimensions smaller than the thickness of the diffusion layer, δ , in a surrounding electrolyte solution. Practically, the size of such sensors can range from several tens of micrometers to nanometers. UMEs can be prepared from different electroactive materials (e.g., carbon, platinum, or gold) using a number of fabrication schemes. Geometry and shape of an electrode can vary depending on the intended application: disks, rings, bands, cylinders, spheres, and hemispheres represent the most common forms.⁴

UMEs have unique properties that make them ideal sensors for biological SECM. Their small size allows for an unhampered approach to cells and provides high lateral resolution for imaging single cells. In addition, UMEs can record very low currents at high S/N.⁵ For example, an appropriate UME along with suitable electronic equipment can measure current signals as low as 30 fA. Also, the applied potential can be altered rapidly (up to 10^6 V s⁻¹) as a result of reduced charging currents. The Ohmic drop of the potential, RI , is relatively small for UMEs because the measured currents are low. Finally, UMEs rapidly reach steady-state conditions, which is a prerequisite for SECM imaging. In the case of a disk UME with a large insulating sheet, the steady-state current, I_{ss} , is defined as

$$I_{ss} = 4n_e F D c r \quad (1)$$

where n_e is the number of electrons involved in the electrochemical process, F is the Faraday constant (9648534×10^3 C mol⁻¹), D is the diffusion coefficient of the electroactive species in solution (m² s⁻¹), c is the concentration of the electroactive species (mol m⁻³), and r is the radius (m) of the electroactive sensor. At steady-state conditions, the sensing zone is precisely defined and localized within a restricted volume at the

Published: January 07, 2011

electrode/solution interface. This implies that the response of the sensor in a homogenized electroactive solution is independent of the actual position until the UME is brought in close proximity to a surface that can interact with its sensing zone. Because the behavior of the UME is affected by mass transport of dissolved electroactive material in the vicinity of the electrode, the presence of a nearby surface can hinder or add to the flux of material detected by the sensor.

In the case of a reversible charge-transfer reaction involving a dissolved electroactive substance, O, the current measured at the UME is proportional to the flux of O, J_o ($\text{mol s}^{-1} \text{m}^{-2}$), at the solution/sensor electrode interface, which is described by Fick's first law as

$$-J_o(x, t) = D_o \partial c_o(x, t) / \partial x \quad (2)$$

where x and t denote positions in space and time, respectively. Fick's first law states that the flux of O is proportional to the concentration gradient, $\partial c_o / \partial x$, at a particular moment and location. For any electrode geometry, the change in concentration of O, ∂c_o , with time is described by Fick's second law as

$$\partial c_o(x, t) / \partial t = D_o \nabla^2 c_o \quad (3)$$

where ∇^2 is the Laplace operator (a differential operator equal to the sum of all the unmixed second partial derivatives of a dependent variable) characteristic of different diffusion geometries. The operator used in the case of linear diffusion to a planar electrode would be different from that of spherical diffusion observed, for example, at a gold sphere electrode.

Equations 2 and 3 reveal that the concentration profile of the reacting electroactive substance depends on both distance from the electrode/solution interface and time. Practically, this relationship implies that by switching the UME's potential from a value at which no electrochemical reaction occurs to that at which O is reduced, O will be consumed, hence c_o will approach zero at the electrode/solution interface ($x = 0$) and $\partial c_o / \partial x$ will develop within a defined region of the bulk solution. The volume of solution in which diffusion of O to the electrode/solution interface occurs is called the diffusion layer and depends on electrolysis time. For planar semi-infinite diffusion, δ is defined as

$$\delta = \sqrt{(\pi D t)} \quad (4)$$

where π is the circular constant (3.14159). To observe UME behavior, the following two conditions must be fulfilled:⁵ 1) the electrolysis time must be sufficient, given the dimensions of the sensor, to reach steady-state conditions and 2) δ/r must be $\gg 1$. At short electrolysis times, small planar UME sensors behave like large planar electrodes. With increasing time, the diffusion layer evolves to its full potential in bulk solution and UME behavior develops. The time necessary to reach steady-state conditions depends on the surface area of the sensor. For example, a sensor with $r = 1 \text{ mm}$ would require $> 4 \times 10^4 \text{ s}$ for 90% of its current signal to be dominated by the steady-state component, whereas a UME with $r = 1 \mu\text{m}$ would achieve steady-state conditions in 0.04 s .⁵

There are two important contributions to the current measured at an electrochemical sensor: 1) linear diffusion (the flux of substance normal to the electrode plane) and 2) hemispherical diffusion (the flux of substance at the edges of the sensor). The latter is responsible for the non-uniform current density commonly measured across an electrode surface. For a large planar sensor, linear diffusion dominates, and the contribution of the

hemispherical diffusion to the overall current is minimal, leading to $\delta/r \ll 1$ and the advent of classical electrode behavior. As the size of the sensor decreases, the contribution of hemispherical diffusion to the overall current increases, and the diffusion-limited flux to the electrode becomes constant with time. The current is proportional to J_o as described in Equation 2, resulting in a steady-state current. This is further related to c_o (Equation 1) because the time derivative of Equation 3 is zero.⁵ This situation occurs for $\delta/r \gg 1$.

■ ULTRAMICROELECTRODES

Electrochemical sensors used to study single cells and cell patterns must 1) have appropriate dimensions, 2) be stable over the time scale of the experiment, 3) be sensitive and selective to the analyte, and 4) provide high S/N. The materials commonly used for the preparation of these sensors include carbon, platinum, and gold. Initially, carbon was the preferred material for cell studies because it was thought to be less susceptible to electrode fouling than platinum and gold, but recent studies using platinum UMEs in extracellular⁶ and intracellular⁷ experiments observed no significant fouling of the metal surface by cell constituents. Arguably, gold sensors would best be used in extracellular studies given the high affinity of sulfur-containing proteins to gold. Gold remains nevertheless an interesting material for the preparation of UMEs mainly because sensor preparation is easy and gold is sensitive to quinone-containing compounds.⁸ The overall sensitivity and selectivity of a UME to an analyte interacting with or originating from a cell is difficult to predict. Carbon electrodes have detected the release of catecholamine neurotransmitters on an individual adrenal gland (PC-12) and chromaffin cells.^{9,10} These cells undergo exocytosis, thereby releasing hormones and neurotransmitters from membrane-bound storage vesicles into the extracellular space.

A carbon UME sensor is obtained by sealing a carbon fiber (CF) with an insulating sheet followed by careful polishing (e.g., in the case of a glass-based seal) or sectioning with a scalpel (e.g., in the case of polymers such as polyethylene, propylene, or electrophoretic paint) to expose the active surface of the sensor. CF-UMEs with diameters of $5\text{--}10 \mu\text{m}$ can be routinely produced, but electrochemical,^{5,11} electrical,¹² flame,^{5,13} or ion beam¹⁴ etching procedures can further reduce the diameter. Modification of the carbon electrode surface (e.g., with complex compounds or enzymes) is often needed to improve the selectivity of the sensor to other important cell analytes, such as nitrogen oxide or glucose.^{15,16} Alteration of electrode properties requires analysis of the sensor response prior to performing electrochemical cell studies.

Bare, disk-shaped platinum UMEs can perform extra- and intracellular measurements of oxygen gas,⁷ reactive oxygen species,¹⁷ and cell metabolites (e.g., thiodione).^{6,8} Such electrodes are typically produced by sealing platinum nano- or micro-wires with thin tapers of pulled glass capillaries.^{18,19} These are created by pulling an annealed platinum wire (e.g., $25 \mu\text{m}$ in diameter) into glass (e.g., borosilicate or quartz) under vacuum using a laser pipette puller. Optimization of pulling parameters can control the shape and size of the sensor. The characteristics of a sensor are largely dependent on the polishing process used to expose the platinum electrode surface. Voltammograms recorded at these sensors are fully retraceable and attain a steady-state current at sweep rates as high as 10 V s^{-1} .⁷ The same methods can produce ultrasharp platinum disk UMEs of

nanometer dimensions. When using a tip radius that is ~ 1000 times smaller than that of a cell, measurements of membrane potentials can be performed without inducing apparent damage (see below).

Electrochemical micropipettes are a relatively new sensor type that is being developed for biological SECM. They consist of glass micropipettes coated with a thin film of gold or platinum. The preparation of electrochemical micropipettes requires several steps. Borosilicate glass capillaries are first pulled using a filament or laser puller. The shape of the resulting pipette depends on the pulling parameters and can be optimized to yield apertures that are $1\text{--}2\text{ }\mu\text{m}$ in diameter with a well-defined taper that is $\sim 0.5\text{ cm}$ in length. The pulled end of the micropipette is then coated with a thin film of gold by thermal evaporation. Micropipettes are rotated at a rate of $\sim 30\text{ rpm}$ at an angle of $20\text{--}50^\circ$ with respect to the surface plane to obtain a uniform gold coating and prevent accumulation of gold at the aperture. Rotation of the micropipettes is maintained throughout the entire evaporation process and during cooling of the evaporation chamber to obtain a smooth and uniform deposit. A fine copper coil and conductive, silver-containing epoxy resin complete the electrical connection to the gold film.^{20,21} To prevent clogging of the capillary during the electrophoretic deposition step, the unmodified end of the micropipette is connected to a source of nitrogen gas at a pressure of 70 Psi. The gold-coated tip of the micropipette is then inserted in a platinum coil immersed in electrophoretic solution to isolate the side walls with a polymer layer (e.g., by chronopotentiostatic deposition). The pipette is finally rinsed and cured by thermal treatment. The micropipette-based electrochemical sensor is typically characterized by scanning electron microscopy (SEM), cyclic voltammetry, and SECM approach curves. Examples of gold-coated micropipettes are shown in Figures 1C and 1D. The diameter of aperture is $\sim 2\text{ }\mu\text{m}$, and the gold film is $50\text{--}80\text{ nm}$ thick and extends to the edge of the opening. Because the thickness of the insulation layer at the pipette aperture is only a few tens of nanometers, a second coating of paint is sometimes necessary to minimize the presence of pinholes in the polymer layer. The nanometer dimensions of the sensors combined with their ability to dispense volumes of solution in the picoliter range near or inside a cell make them attractive candidates for cell transport studies. In the past, micropipettes have been reported in ion-selective electrode studies that monitor ion-transfer reactions.^{22,23} Micropipettes can also be filled with enzymes to probe the catalytic activity of a surface²⁴ or be used for microdispensing experiments in conjunction with scanning chemiluminescence microscopy.^{25,26} The deposition of a defined electroactive layer on the outside of a micropipette allows for simultaneous solution dispensing and electrochemical detection. The electrochemical behavior of the micropipettes is well defined and follows the steady-state current expected for a ring electrode. The SECM approach curves are also consistent with theory.²⁰ The dispensing capabilities of electrochemical micropipettes²⁰ promote injection of electroactive species into a cell or generation of a constant flow of a solution in close vicinity, allowing drugs or other agents to stimulate a response from the cell.

INSTRUMENTATION

In SECM, the UME is scanned over a surface using a high-resolution positioning system. During movement of the electrode, the steady-state current is monitored continuously.

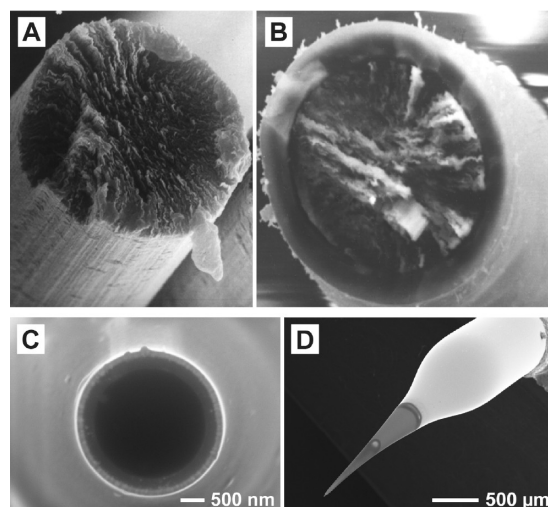


Figure 1. SEM images of the tips of A) bare and B) insulated carbon fibers that are $10\text{ }\mu\text{m}$ in diameter. The insulating material is a thin layer of electrodeposition paint, which covers the side walls but not the disk-shaped face of the carbon fiber. The electrode surface has been exposed by carefully sectioning the sealed carbon fiber with a scalpel blade. The resulting CF-UME is typically used for neurotransmitter and hormone release measurements on single secretory cells. Reproduced with permission from ref. 9. Copyright 2007, Wiley-VCH. C) Top view and D) side view of an insulated 70-nm-thick gold ring micropipette. The insulating material is a thin layer of cathodic electrophoretic paint, which covers the sides but not the ring face of the micropipette. The remainder of the gold coated film is insulated with a varnish prior to electrochemical measurements. The resulting gold ring micropipet can dispense pL volumes through its orifice.

Steady-state current is observed when the electrochemical reaction of a dissolved reversible redox species at the UME/solution interface is mass transfer limited for potentials far exceeding the redox potential of the species. Given the unique properties of UMEs,²⁷ the detection of the topography and/or reactivity of a nearby surface occurs within the localized hemispherical diffusion zone of the species. Monitoring the extent by which the diffusion of species from surface features is hindered reveals surface topography. Large features significantly disrupt diffusion to the UME and alter the localized hemispherical diffusion zone such that current decreases. Surface reactivity is evaluated from localized increases in current that are related to the kinetics of species regenerated at the sample surface. There are other important parameters that affect SECM responses, such as UME geometry, the UME-to-surface distance, and the RG factor, which is the ratio of the radii of insulating material and metal wire.¹

Both topography and/or reactivity of the sample surface affect UME currents in SECM experiments; hence, unambiguous interpretation of SECM imaging studies requires deconvolution of each contribution. In the case of an SECM approach curve, in which the UME is approached normal to the sample surface, deconvolution of the SECM response is not necessary, as long as the UME is much smaller than the sample surface features. SECM imaging in which the UME is positioned within a few tip radii of the sample surface and scanned parallel to the surface plane commonly employs two experimental strategies—constant-height and constant-distance (Figure 2A). In constant-height imaging, the UME is scanned over a surface in both x - and y -directions at a fixed vertical distance (z -direction).

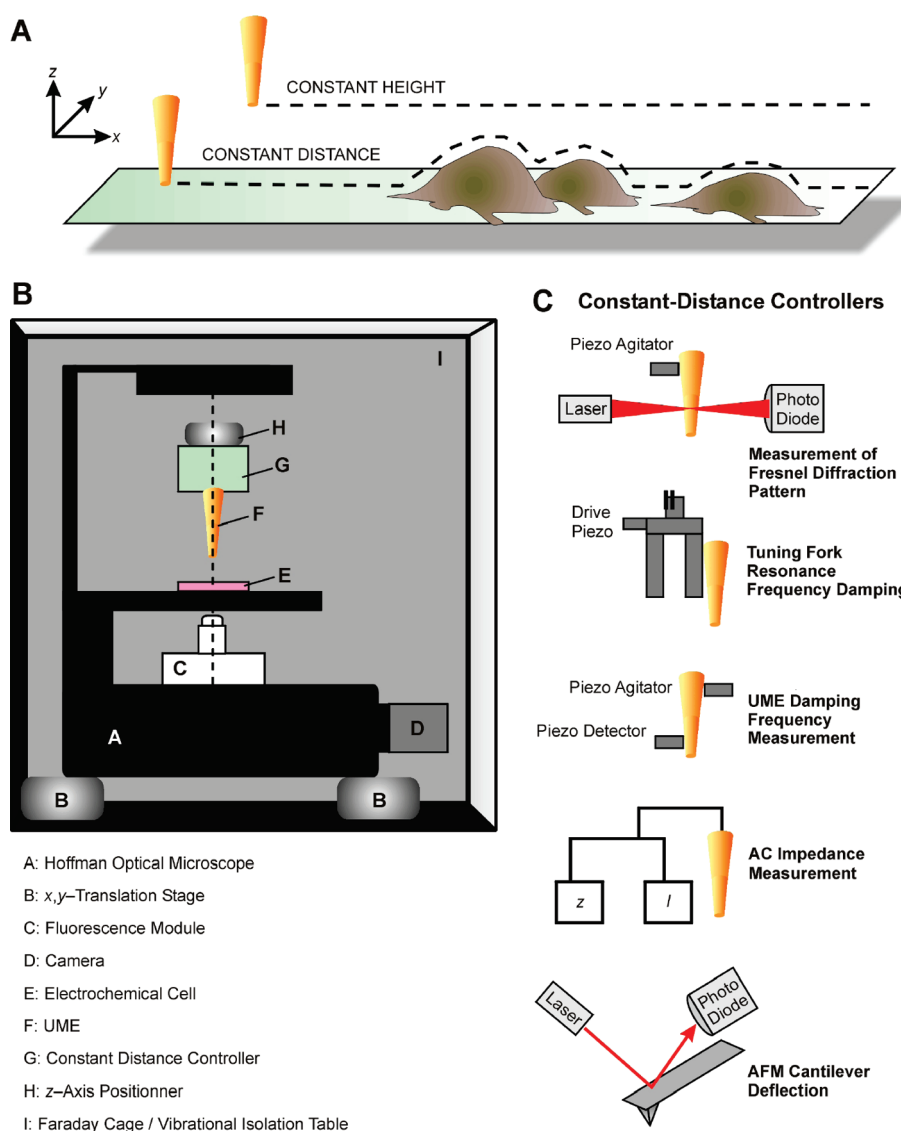


Figure 2. A) Schematic presentation of an SECM line scan over immobilized cells in constant-height and constant-distance mode. B) Instrumental design of a Bio-SECM. C) Examples of constant-distance controllers and their detection principles.

Constant-height imaging can be readily applied to smooth and planar samples for which features do not exceed preset values in height, as is the case for self-assembled monolayers of alkanethiols on gold.²⁸ Although instrumentally easier to implement, constant-height imaging is prone to tip-sample crashes when the preset height is reduced to achieve better resolution. Therefore, constant-height mode imaging is unlikely to be used significantly in SECM studies of biological samples, especially when large aspect-ratio features, such as cells, are the subject of investigation. Constant-distance SECM imaging, on the other hand, uses an additional feedback control mechanism to maintain a constant UME-to-sample distance, making it possible to deconvolute surface topography from its electrochemical activity. At present, constant-distance imaging mode is widely accepted as the norm for SECM studies with immobilized cells.

The concept of Bio-SECM emerged after several groups combined conventional SECM with an inverted microscope to build an instrument suitable for studying local electrochemical reactions at immobilized cells.^{6–8,29–31} The inverted microscope confers several advantages to cell studies, including quick identi-

fication of healthy cells based on morphological changes and prepositioning of the UME close to cells, which reduces overall experimental time. Cell activity in the context of an SECM experiment is difficult to define and can imply the need for both direct and indirect modes of electrochemical detection. Direct detection is generally applied to cell constituents (e.g., a neurotransmitter), cell metabolites (e.g., thiodione), or cell functions (e.g., respiration). Indirect detection methods may be employed when direct measurements are difficult to perform, as is the case for several cell properties (e.g., the intracellular redox potential of a cell) and reactions occurring at its surface.

As an example, Figure 2B shows a schematic of the instrumental setup of a selected Bio-SECM manufactured by HEKA Elektronik Dr. Schulze GmbH (Lambrecht/Pfalz, Germany). The instrument employs an inverted microscope comprising adapted optics for cell imaging such as Hoffman modulation contrast to visualize cell morphology and quickly identify healthy cells prior to performing electrochemical measurements. The microscope is also equipped with a fluorescence module and a CCD camera to perform toxicology and viability measurements

simultaneously during or following SECM imaging. The entire microscope system is mounted on an x,y -translocation stage to align the optical axis of the microscope with the UME. The UME is placed above the immobilized cell substrate residing in a specially designed electrochemical cell that also accommodates reference and auxiliary electrodes. The UME is connected to a constant-distance controller that regulates the UME-to-cell distance during imaging. The setup is placed on a vibration-damping table enclosed in a Faraday cage to shield the instrument against acoustic and electrical interference during measurements and improve fluorescence-imaging conditions.

■ PRINCIPLES OF CONSTANT-DISTANCE POSITIONING

To achieve optimal sensitivity and resolution in an SECM measurement, the sensor should be moved as close as possible over the sample while maintaining constant distance to the surface. Maintaining a constant UME-to-sample distance during SECM imaging generally relies on computer-controlled feedback circuitry to monitor the position of the UME, compare it with a preset value, and make adjustments when deviations occur. Figure 2C presents examples of constant-distance positioning schemes that proved suitable for SECM instrumentation, including various forms of shear-force control, AC impedance measurements, and cantilever deflection mechanisms.

Shear force based distance controllers rely on the detection of short-range (e.g., 100–200 nm) hydrodynamic forces between the sample and a vibrating UME that approaches the surface at a predefined resonance frequency. A piezoelectric agitator stimulates the probe, and damping of the resonance frequency by the viscous drag of liquid between the UME and the surface provides feedback for the SECM positioning system to maintain a constant UME-to-sample distance. A beam of laser light that is focused on the UME and projecting the Fresnel diffraction pattern onto a split photodiode can optically detect frequency damping.³² Another concept of feedback control, which was originally developed for near-field scanning optical microscopy, involves a tuning fork vibrated by a piezoelectric buzzer. The UME is fixed on one leg of the fork, and the resonance frequency of the tuning fork produces an AC voltage output that is sensitive to the presence of shear forces between the UME and the surface.^{31,33} Piezoelectric plates can also excite the UME at a resonance frequency and detect the amplitude of the UME vibration.³⁴ This scheme is employed in the instrument presented in Figure 2B.

Alternative approaches rely on recording UME current generated by dissolved electroactive species to provide feedback for constant-distance imaging.³³ Possible strategies include both maintaining constant amperometric tip current³⁰ and impedance measurements.^{17,35,36} In the latter case, UME impedance is modulated to high frequencies (e.g., ~50 kHz) to distinguish it from Faraday processes that occur at lower frequencies. Simpler to implement than shear-force methods, UME impedance can monitor cell morphology and substrate topography in a medium that is free of redox species. However, impedance-based methods are susceptible to local impedance variations during certain biological processes such as vesicular release,³⁷ and the resolution is typically lower than that obtained with competing concepts, such as constant-current imaging. Conceptually related, ion conductance^{38,39} is another promising strategy for feedback control. This method employs an electrochemical micropipette

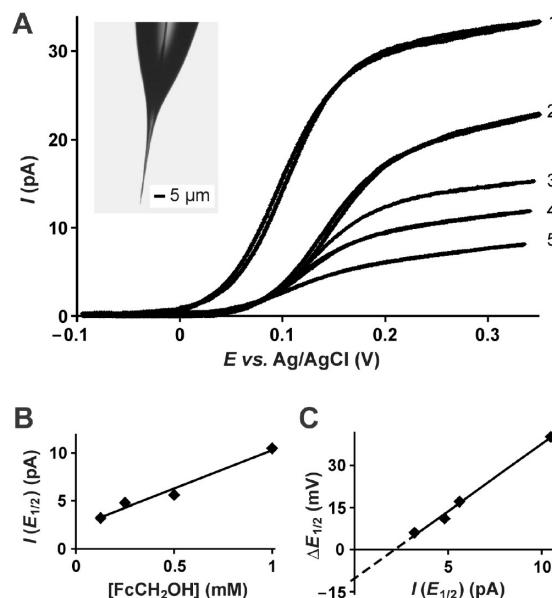


Figure 3. A) Voltammograms of FcCH_2OH oxidation at a 112-nm platinum tip obtained in bulk solution (curve 1) and inside a human breast epithelial (MCF-10A) cell (curves 2–5). The following concentrations of FcCH_2OH were used: 1.0 mM for curves 1 and 2, 0.5 mM for curve 3, 0.25 mM for curve 4, and 0.125 mM for curve 5. The inset shows an optical micrograph of a laser-pulled platinum disk UME. B) Dependence of the UME current at half-wave potential, $I(E_{1/2})$, on $[\text{FcCH}_2\text{OH}]$. C) Dependence of the change in half-wave potential, $\Delta E_{1/2}$, on $I(E_{1/2})$. Reproduced with permission from ref. 7. Copyright 2008, The National Academy of Sciences U.S.A.

as the sensor, and variation in ion flow indicates whether the probe is approaching or retracting from a sample surface.

The use of specialized cantilevers in conjunction with atomic force microscopy (AFM) instrumentation proved suitable for achieving high-resolution SECM imaging.⁴⁰ Here, the tip of the cantilever serves as both UME and force sensor to monitor current and topography simultaneously. Drawbacks of combined SECM/AFM strategies include relatively long acquisition times, the need to modify the surface of cantilevers, and limited robustness.

The controllers described in this section all strive to master constant-distance SECM measurements performed on soft substrates such as cells. Soft substrates are technically more challenging to probe than rigid ones (e.g., the surface of a metal film) because their interfaces are less confined. Therefore, shear force methods are nontrivial to apply to biological systems such as live cells since interaction of the probe and the sample are often unstable, compromising precision of the feedback signal. Cells are also likely to deform upon contact with the UME, which may occur in the case of shear-force positioning systems that require UME–sample separation of a few hundred nanometers. The impact of contact on frequency damping is unclear, yet should vary significantly with the type of UME that is being used.²⁹

■ SELECTED DEMONSTRATIONS

The capacity of SECM to probe and elucidate biochemical events related to cellular activity has been demonstrated in a number of ways, and several excellent review articles have been devoted to this field.^{9,10,41,42} Among the diverse range of applications, SECM has probed membrane permeability,^{7,43} detected

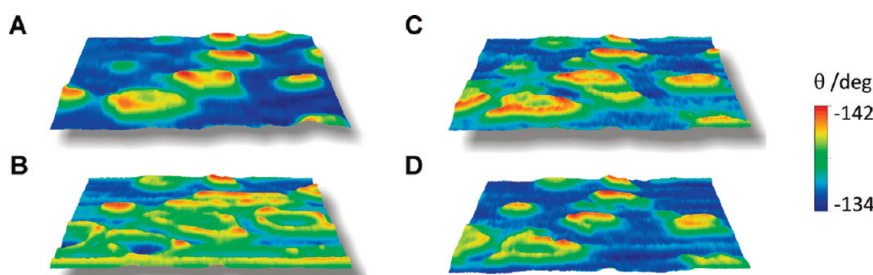


Figure 4. AC-SECM images (phase shift vs SECM probe position) obtained above a confluent layer of Cos-7 cells A) before PMA stimulus; B) immediately after addition of PMA; C) 6 min after PMA stimulus; and D) 12 min after PMA stimulus. Images in modified form are adapted from ref. 44 with permission from RSC and were obtained through the courtesy of Prof. Zhifeng Ding (The University of Western Ontario). Copyright 2007, Royal Society of Chemistry.

the presence of metabolites,^{15,44} and evaluated enzymatic activity.^{45,46} A few recent examples are briefly discussed below.

The potential of a cell membrane can be estimated by measuring voltammograms at a platinum UME sensor inside and outside a cell (Figure 3). When human breast epithelial cells (MCF-10A) are exposed to a solution of a hydrophobic redox substance, such as 1-(ferrocenyl)methanol (FcCH_2OH), partition of the substance occurs between the extra- and intracellular domains. Using this effect, Mirkin and coworkers have measured a difference of 36 mV between the half-wave potentials ($\Delta E_{1/2}$) for FcCH_2OH oxidation, which can be attributed to the potential drop across the cell membrane of the MCF-10A cells.⁷ Experiments with different UMEs produced a mean $\Delta E_{1/2}$ of 46 ± 4 mV (for $n = 18$ at the 95% confidence interval). The addition of depolarizing agents (e.g., 600 nM valinomycin) to the solution was expected to diminish the membrane potential. In each of the experiments performed on MCF-10A cells in the presence of valinomycin, $\Delta E_{1/2}$ decreased markedly, and an average value of $\Delta E_{1/2} = 16.7$ mV was observed for FcCH_2OH mediator. Although there is some variability in the membrane potential values reported in the literature, measured average values for $\Delta E_{1/2}$ are somewhat higher than most numbers obtained for mammalian cells by different electrochemical techniques (e.g., -58.6 mV vs. -2.7 mV reported for MCF-7 human mammary tumor cells).⁴⁷

The Ohmic potential drop across the membrane, RI , with R being the membrane resistance ($\text{G}\Omega$), is proportional to I flowing at the tip of the electrode inserted in the cell. The voltammograms in Figure 3A represent the platinum UME's response in a bulk solution of FcCH_2OH outside the cell (curve 1) and inside the same cell (curves 2–5) for different concentrations of FcCH_2OH . Varying the concentration of FcCH_2OH in solution reveals a linear dependence of the tip current corresponding to the half-wave potential, $I(E_{1/2})$ (Figure 3B). The $\Delta E_{1/2}$ value decreased upon dilution while the plot of $\Delta E_{1/2}$ vs. $I(E_{1/2})$ remains linear (Figure 3C). The membrane resistance extracted from the slope of the graph is $\sim 4 \text{ G}\Omega$. Interpolation of the plot reveals a membrane potential corrected for the polarization effect of about -10 mV, which is in good agreement with values that were reported earlier.⁴⁷ Although more in-depth work is required, the use of intracellular voltammetry to measure membrane potentials is a relatively straightforward technique that could easily be applied to several different kinds of cell cultures.

Alternating current (AC)-SECM can perform measurements without any supplementary redox species in the solution. This is especially important for studies of biological samples when

the presence of electroactive species, which are often toxic, is not desired. Only minor modifications of a typical SECM setup are required for AC-SECM. The dependence of AC magnitude on tip-to-sample separation distance can determine cell topography and monitor real time changes in cell height of individual cells. Moreover, AC-SECM can observe changes in metabolic cellular activity. For example, Ding and coworkers⁴⁴ performed AC-SECM experiments to monitor the oxidative burst of a confluent layer of Cos-7 cells induced by the addition of phorbol-1,2-myristate-acetate-3 (PMA). Figure 4A demonstrates an AC-SECM image (phase shift vs. SECM probe position) obtained in cell culture medium above the cells before addition of PMA. Next, the cells were stimulated by adding PMA to the medium, which increased production of reactive oxygen species and changed the phase shift of the AC current at the SECM probe (Figure 4B). Additional AC-SECM images obtained 6 and 12 min after the PMA stimulus (Figures 4C and 4D, respectively) indicate decreasing intensity of the cellular respiration.

More recently, Matsue and coworkers estimated the density of membrane protein without detaching a cell from its dish (Figure 5).⁴⁶ The current response trends of different cells agreed with flow cytometry results, which indicated that the membrane protein of patterned cells is detectable. To do so, they used an SECM-based ELISA with alkaline phosphatase (ALP) as a labelling enzyme on the epidermal growth factor receptor (EGFR), a relevant target in cancer therapy responsible for abnormal cell proliferation. ALP hydrolyzes *p*-aminophenylphosphate monosodium salt (PAPP) into *p*-aminophenol (PAP) (Figure 5A), and the researchers could detect the production of PAP while the potential was fixed at 0.3 V vs. Ag/AgCl. Using a generation-collection mode, they compared the response in a CHO cell with and without EGFR in its membrane (Figure 5B). They found that the current was much higher in the EGFR/CHO cell, showing the possibility of detecting EGFR expression level at the single cell scale. These results underline the great potential of SECM as a promising tool in cell studies.

CONCLUSION AND OUTLOOK

SECM has become a useful method to reveal chemical or biochemical events occurring on or in close proximity to a surface. The technique records the electrochemical response as a UME moves towards or over a sample using precise positioning and feedback systems. Electrochemical detection is specific because detected molecules undergo electron transfer reactions at well-defined potentials. UMEs provide current sensitivity in the pA regime, making it possible to detect even trace amounts of

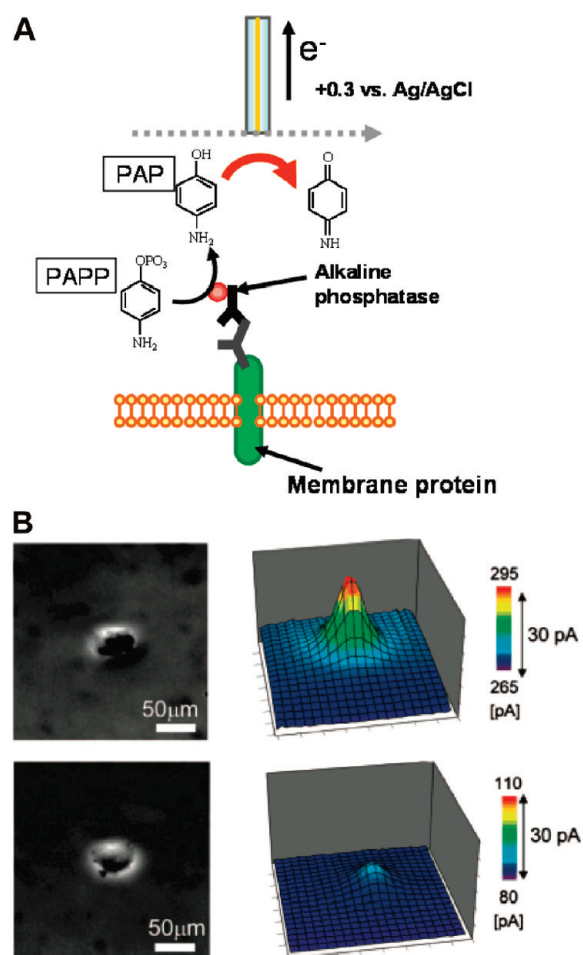


Figure 5. A) Schematic representation of EGFR detection using generation-collection mode. The redox current indicates the density of membrane protein on the cellular surface. B) Optical micrographs (left-hand panels) and SECM images (right-hand panels) of single living mammalian cells, one of which is overexpressing EGFR (top panels) while the other (normal CHO) serves as a control sample (bottom panels). The electrode was $15\ \mu\text{m}$ above the substrate, and the scan rate was $5\ \mu\text{m s}^{-1}$. The scan range was $200 \times 200\ \mu\text{m}^2$, and the step size was $5\ \mu\text{m}$. Reproduced from ref. 46.

analytes rapidly and with high spatial control. Unlike macroelectrodes, UMEs are largely insensitive to convection and quickly reach steady-state conditions (e.g., in the range of micro- to milliseconds) following the application of a potential step. They can therefore be considered steady-state systems when moving through the solution. These properties are critical for SECM imaging applications and the determination of local concentration of redox species diffusing into, being released from, or interacting with cells.

Routine fabrication of nanoprobe for high sensitivity measurements is a prerequisite for the study of cells using SECM. The selection of a proper sensor material is important with respect to the nature of the analyte to be detected. Proof-of-concept studies have demonstrated the ability of electrochemical sensors to image and quantify transport processes for a variety of cell lines. Development of Bio-SECM as a bioanalytical tool capable of following cell metabolism also depends on advances in instrumental design, the availability of suitable biocompatible cell supports, and the routine use of cytotoxicity measurements.

Constant-distance controllers in SECM instrumentation are important for decoupling the cell's topography from its electrochemical activity. Several types of feedback control systems have been tested to this end, yet successful application of constant-distance controllers remains challenging when used in conjunction with soft, deformable substrates such as live cells.

Microfabrication techniques hold promise in supporting SECM-based investigation by providing fluidic-based culture platforms that can control cell environments at well-defined length scales.⁴⁸ Plastic polymers as supports for cell growth further offer the possibility of tuning size, shape, and topography of the substrate through molding or embossing techniques. Fluorescence-based cell status assays may be required prior to SECM experiments, presenting a convenient and reliable approach to assess the impact of lithographic processing and the compatibility of synthetic materials with live cells.⁴⁹ Integration of an inverted fluorescence microscope with SECM also allows simultaneous or subsequent evaluation of the state of the cells following SECM measurements.

When performing electrochemical measurements in the presence of cells, it is important to equilibrate maintenance of the sample and probe stability. Biomolecules from the cell culture medium or even cells themselves can irreversibly bind to the UME, thereby compromising its sensitivity. An option is to modify the medium, but changing one of the experimental components, such as medium or temperature, always necessitates tests to ensure that the cell feature studied is not altered such that a different electrochemical behavior would be observed. Here, we see potential for further development of routine protocols that aim to improve reliability of SECM as an analytical tool.

Bio-SECM has the potential to quantify how important biological electroactive molecules work together, are transported in and out of cells, and can positively contribute to the global approach of cellular studies called systems biology. In the future, SECM is likely to have a direct impact on the design of drugs and pharmaceutical targets, especially when performed in conjunction with complementary analytical methods and techniques. Therefore, much interest remains in developing integrative microscopy techniques capable of monitoring and studying specific metabolites and proteins with high spatial resolution for both single cell and monolayer cultures. Such experiments will provide further insights into some of the unresolved mysteries surrounding life at the molecular and cellular level.

ACKNOWLEDGMENT

We are grateful to Tomokazu Matsue (Tohoku University), Wolfgang Schuhmann (Ruhr-Universität Bochum), Zhifeng Ding (The University of Western Ontario), Michael V. Mirkin (Queens College—City University of New York), Damien Marchal (Université Paris Diderot), and Stephan Borensztajn (Université Paris Diderot) for their assistance. We thank Robert Gates (Sigma-Aldrich Corp.) for designing the artwork on Bio-SECM.

BIOGRAPHIES

Isabelle Beaulieu, M.Sc., is a Technical Officer with the National Research Council of Canada at the Biotechnology Research Institute in Montréal. Matthias Geissler, Ph.D., is a Research Officer with the National Research Council of Canada at the Industrial Materials Institute in Boucherville, and an

adjunct professor at the Chemistry Department at the University of Québec in Montréal. Sabine Kuss is a graduate student in the Mauzeroll research group. Janine Mauzeroll, Ph.D., is an associate professor with the Chemistry Department at the University of Québec in Montréal. Address correspondence to Mauzeroll at mauzeroll.janine@uqam.ca.

REFERENCES

- (1) Bard, A. J.; Fan, F.-R. F.; Kwak, J.; Lev, O. *Anal. Chem.* **1989**, *61*, 132–138.
- (2) *Scanning Electrochemical Microscopy*; Bard, A. J.; Mirkin, M. V., Eds.; Marcel Dekker: New York, NY, 2001.
- (3) Sun, P.; Laforge, F. O.; Mirkin, M. V. *Phys. Chem. Chem. Phys.* **2007**, *9*, 802–823.
- (4) *Handbook of Electrochemistry*; Zoski, C. G., Ed.; Elsevier Science: Amsterdam, The Netherlands, 2007.
- (5) Štulík, K.; Amatore, C.; Holub, K.; Mareček, V.; Kutner, W. *Pure Appl. Chem.* **2000**, *72*, 1483–1492.
- (6) Mauzeroll, J.; Bard, A. J.; Owhadian, O.; Monks, T. J. *Proc. Natl. Acad. Sci. U. S. A.* **2004**, *101*, 17582–17587.
- (7) Sun, P.; Laforge, F. O.; Abeyweera, T. P.; Rotenberg, S. A.; Carpino, J.; Mirkin, M. V. *Proc. Natl. Acad. Sci. U. S. A.* **2008**, *105*, 443–448.
- (8) Mauzeroll, J.; Bard, A. J. *Proc. Natl. Acad. Sci. U. S. A.* **2004**, *101*, 7862–7867.
- (9) Schulte, A.; Schuhmann, W. *Angew. Chem.* **2007**, *46*, 8760–8777.
- (10) Wightman, R. M. *Science* **2006**, *311*, 1570–1574.
- (11) Chen, S.; Kucernak, A. *Electrochem. Commun.* **2002**, *4*, 80–85.
- (12) Millar, J.; Pelling, C. W. A. *Journal of Neuroscience Methods* **2001**, *110*, 1–8.
- (13) Strein, T. G.; Ewing, A. G. *Anal. Chem.* **1992**, *64*, 1368–1373.
- (14) Zhang, X.; Zhang, W.; Zhou, X.; Ogorevc, B. *Anal. Chem.* **1996**, *68*, 3338–3343.
- (15) Taha, Z. H. *Talanta* **2003**, *61*, 3–10.
- (16) Yao, D. D.; Vlessidis, A. G.; Evmiridis, N. P. *Microchimica Acta* **2004**, *147*, 1–20.
- (17) Diakowski, P. M.; Ding, Z. *Electrochem. Commun.* **2007**, *9*, 2617–2621.
- (18) Katemann, B. B.; Schuhmann, W. *Electroanalysis* **2002**, *14*, 22–28.
- (19) Mauzeroll, J.; LeSuer, R. J. In *Handbook of Electrochemistry*; Zosky, C. G., Ed.; Elsevier Science: Amsterdam, The Netherlands, 2007; pp 199–211.
- (20) Walsh, D. A.; Fernández, J. L.; Mauzeroll, J.; Bard, A. J. *Anal. Chem.* **2005**, *77*, 5182–5188.
- (21) Demaille, C. In *Handbook of Electrochemistry*; Zosky, C. G., Ed.; Elsevier Science: Amsterdam, The Netherlands, 2007; pp 226–235.
- (22) Liu, B.; Shao, Y.; Mirkin, M. V. *Anal. Chem.* **2000**, *72*, 510–519.
- (23) Yuan, Y.; Amemiya, S. *Anal. Chem.* **2004**, *76*, 6877–6886.
- (24) Hengstenberg, A.; Kranz, C.; Schuhmann, W. *Chem.—Eur. J.* **2000**, *6*, 1547–1554.
- (25) Kasai, S.; Zhou, H.; Matsue, T. *Chem. Lett.* **2000**, *29*, 200–201.
- (26) Hirano, Y.; Mitsumori, Y.; Oyamatsu, D.; Nishizawa, M.; Matsue, T. *Biosens. Bioelectron.* **2003**, *18*, 587–590.
- (27) Amatore, C. In *Electrochemistry at Microelectrodes*; Rubinstein, I., Ed.; Marcel Dekker: New York, NY, 1995; pp 131–208.
- (28) Liu, B.; Bard, A. J.; Mirkin, M. V.; Creager, S. E. *J. Am. Chem. Soc.* **2004**, *126*, 1485–1492.
- (29) Bauermann, L. P.; Schuhmann, W.; Schulte, A. *Phys. Chem. Chem. Phys.* **2004**, *6*, 4003–4008.
- (30) Kurulugama, R. T.; Wipf, D. O.; Takacs, S. A.; Pongmayteegul, S.; Garriss, P. A.; Baur, J. E. *Anal. Chem.* **2005**, *77*, 1111–1117.
- (31) Takahashi, Y.; Hirano, Y.; Yasukawa, T.; Shiku, H.; Yamada, H.; Matsue, T. *Langmuir* **2006**, *22*, 10299–10306.
- (32) Ludwig, M.; Kranz, C.; Schuhmann, W.; Gaub, H. E. *Rev. Sci. Instrum.* **1995**, *66*, 2857–2860.
- (33) Lee, Y.; Ding, Z.; Bard, A. J. *Anal. Chem.* **2002**, *74*, 3634–3643.
- (34) Katemann, B. B.; Schulte, A.; Schuhmann, W. *Chem.—Eur. J.* **2003**, *9*, 2025–2033.
- (35) Ervin, E. N.; White, H. S.; Baker, L. A.; Martin, C. R. *Anal. Chem.* **2006**, *78*, 653–6541.
- (36) Gabrielli, C.; Huet, F.; Keddad, M.; Rousseau, P.; Vivier, V. *J. Phys. Chem. B* **2004**, *108*, 11620–11626.
- (37) Yamada, H.; Fukumoto, H.; Yokoyama, T.; Koike, T. *Anal. Chem.* **2005**, *77*, 1785–1790.
- (38) Comstock, D. J.; Elam, J. W.; Pellin, M. J.; Hersam, M. C. *Anal. Chem.* **2010**, *82*, 1270–1276.
- (39) Takahashi, Y.; Shevchuk, A. I.; Novak, P.; Murakami, Y.; Shiku, H.; Korchev, Y. E.; Matsue, T. *J. Am. Chem. Soc.* **2010**, *132*, 10118–10126.
- (40) Fasching, R. J.; Bai, S.-J.; Fabian, T.; Prinz, F. B. *Microelectron. Eng.* **2006**, *83*, 1638–1641.
- (41) Yasukawa, T.; Kaya, T.; Matsue, T. *Electroanalysis* **2000**, *12*, 653–659.
- (42) Bard, A. J.; Li, X.; Zhan, W. *Biosens. Bioelectron.* **2006**, *22*, 461–472.
- (43) Cai, C.; Liu, B.; Mirkin, M. V.; Frank, H. A.; Rusling, J. F. *Anal. Chem.* **2002**, *74*, 114–119.
- (44) Diakowski, P. M.; Ding, Z. *Phys. Chem. Chem. Phys.* **2007**, *9*, 5966–5974.
- (45) Lei, R.; Stratmann, L.; Schäfer, D.; Erichsen, T.; Neugebauer, S.; Li, N.; Schuhmann, W. *Anal. Chem.* **2009**, *81*, 5070–5074.
- (46) Takahashi, Y.; Miyamoto, T.; Shiku, H.; Asano, R.; Yasukawa, T.; Kumagai, I.; Matsue, T. *Anal. Chem.* **2009**, *81*, 2785–2790.
- (47) Wonderlin, W. F.; Woodfork, K. A.; Strobl, J. S. *J. Cell. Physiol.* **1995**, *165*, 177–185.
- (48) El-Ali, J.; Sorger, P. K.; Jensen, K. F. *Nature* **2006**, *442*, 403–411.
- (49) Beaulieu, I.; Geissler, M.; Mauzeroll, J. *Langmuir* **2009**, *25*, 7169–7176.